Robotica (2002) volume 20, pp. 13–22. © 2002 Cambridge University Press
DOI: 10.1017/S0263574701003587 Printed in the United Kingdom

A novel articulated mechanism mimicking the motion of index fingers

Giorgio Figliolini and Marco Ceccarelli

Laboratory of Robotics and Mechatronics, DiMSAT – University of Cassino, Via G. Di Biasio, 43 – 03043 Cassino (FR), (ITALY)
E-mail: figliolini@unicas.it
E-mail: ceccarelli@unicas.it

(Received in Final Form: April 25, 2001)

SUMMARY
In this paper we propose an analytical formulation for simulation and design of a one d.o.f. articulated finger mechanism with three phalanges. The formulation is based on a study of the design and operation of an index human finger. In particular, we have proposed a suitable mechanical design for an anthropomorphic finger as both an approximation of human architecture and an easy practical design. Kinematic characteristics are illustrated with numerical examples.

KEYWORDS: Robotics; Hands; Articulated fingers; Kinematic analysis; Design.

I. INTRODUCTION

The design of multifingered robotic and prosthetic hands is aimed to develop mechatronic devices, which can mimic the performance of a human hand. The optimal grasping capabilities of a human hand allow versatile functionality and interaction with several environments. This capability to perform many types of grasp has suggested useful classifications for designing suitable artificial hands. Several papers on this topic refer to six types of grasps that were defined by Schlesinger:[1] cylindrical, fingertip, hook, palmar, spherical and lateral. A taxonomy of manufacturing grasps is obtained by two basic categories, which are defined as power grasps and precision grasps, respectively. An expert system has been formulated for choosing grasps from input information about object shape and required task.[2] More recently, human prehension has been explored in order to develop the design and control of dexterous robot hands.[3]

A suitable knowledge of the anatomy and mechanics of the human hand is required in order to emulate its main performance. An accurate description of the basic structure of bones and neuromuscular apparatus for motion and force control can be found in reference [1].

A mechanical model of the human hand during the grasp has been formulated for designing and building a prototype with two fingers and a palm.[4] Each phalanx has been connected to the next by means of a revolute joint and each finger motion was obtained through the action of a spring and wire, which reproduce the actions of extensor and flexor human tendons, respectively.

A mechanism consisting of multi-link and series of pulleys has been designed and built for a two fingers versatile robot hand.[5] A suitable pair of antagonist wires is used for the gripping and release movements of each finger.

Significant tendon operated hands are the Standford/JPL hand and the Utah/MIT hand.[6,7] The Standford/JPL hand consists of three articulated fingers with two phalanges and three d.o.f.s for each of them. The Utah/MIT hand has three four d.o.f.s fingers and one four d.o.f. thumb. The actuation system of all fingers has been remotely located by using tendon-operated transmission.

Another example of a tendon-operated hand is that by Manus Colobi.[8] The three fingers are installed on the palm along the vertices of an equilateral triangle. Each finger has been provided with a passive system to return to an extended configuration after any closing movement.

The five articulated fingers of the Belgrade/USC hand are actuated through a single electric motor. It has been designed for simple control rather than to increase its dexterity and flexibility. However, this prototype has been the starting point for the mechanical design of the Cantebury hand. This six-fingered hand has been designed for robotic applications by using across four-bar linkages for its two d.o.f. articulated fingers.[9]

Recently, a prototype of a DLR's multi-sensory articulated four-finger hand has been built with all actuators and sensors directly integrated in the hand's palm or fingers. The movements of median and distal phalanges for each finger have been coupled by giving them one d.o.f. and they have been added to the two d.o.f.s of the proximal phalange.[10]

A mechatronic design of multi-fingered robotic and prosthetic hands can be obtained through careful mechanical design. In fact, good performances in terms of versatility and flexibility can be obtained using suitable mechanical devices. Interesting examples are given by under-actuated grippers or hands, which are defined as those with more d.o.f.s than actuators. A three finger under-actuated hand has been designed and built at Laval University in Québec, Canada.[11,12] Each finger has been provided with four d.o.f.s and two actuators. Three d.o.f.s with only one actuator are used for the closing movement of finger and the fourth d.o.f. is used for the rotation of finger about an axis orthogonal to the palm. The linkage of each

finger is suitable for the grasping of a wide variety of objects with large forces.

This design philosophy can also be found in reference [13], where a prosthetic hand with three fingers has been operated by a single actuator. The shape self-adaptability of this hand has been obtained by means of a multi-functional palm mechanism with three operating positions and an automatically variable speed transmission.

This paper deals with the mechanical design of a one d.o.f. articulated finger mechanism for a robotic hand. A simple procedure is proposed to determine the rotation angles between proximal phalanx and palm, proximal and median phalanges, and median and distal phalanges of the index human finger. Then, the rotation angles of median and distal phalanges have been expressed as a function of the rotation angle of the proximal phalanx. Consequently, an "internal synergy" can be obtained for the finger mechanism, when it is defined as the coupling of the motion of the three phalanges.[13]

The motion analysis of index human finger has been used to design a suitable articulated finger mechanism, which is also the result of previous investigations.[14–17] Thus, we propose a one d.o.f. articulated finger mechanism, which is provided with timing belts and epicyclic gear trains in order to transmit the motion from the proximal to the median and distal phalanges. An anthropomorphic finger prototype has been built and preliminary experimental tests have been carried out at Laboratory of Robotics and Mechatronics in Cassino. Moreover, it is worth noting that, although the proposed anthropomorphic finger prototype has only one d.o.f., different trajectories of the fingertip and different rigid motions of each phalanx can be obtained when few components of the transmission system are substituted because of their easy interchangeability.

A MOTION ANALYSIS OF INDEX HUMAN FINGER

A closing movement of a human finger can be obtained in several ways since one can consider the finger as provided with three d.o.f.s. Robotic finger motions can be very similar to those of a human finger when the robotic finger is controlled by a human finger directly.[18]

The three d.o.f.s can be used together or separately in order to grasp different objects in several ways. However, one can find that the rotation of each phalanx is not completely independent because of the natural closing movement of a human finger. Thus, we have focused our attention on this type of movement with the aim of finding a sequence of human finger configurations, which can be performed by an articulated finger mechanism with one d.o.f. only. For several industrial and prosthetic applications, a smaller versatility and flexibility with respect to a human finger can be greatly compensated by easier actuation and control.

Several methods to detect human finger motion can be found in the literature. For example, an image processing system combining high speed photogrammetry with current measurements has been used by Guo and his co-workers.[19] A device for measuring joint angles of hands, termed "Exos Dextrous Hand Master System", has been applied in reference [20].

A motion analysis of a human finger is required in order to find a suitable kinematic model for its natural closing movement with only one d.o.f.

In this paper a motion analysis for a natural closing movement of an index human finger has been carried out in a simple way by using a sequence of photos taken by means of high-speed camera, as shown in Fig. 1. The dimensions of the phalanges for the index human finger of Fig.1 have been identified as $L_1 = 48$ mm, $L_2 = 28$ mm, $L_3 = 23$ mm, respectively. Referring to Fig. 1, the joints between proximal phalanx and palm, proximal and median phalanges, median and distal phalanges have been suitably marked in order to record with good approximation the rotation of each phalanx. In particular, the six photos of Fig. 1 show the following: The initial fully extended configuration (I); a starting movement of the finger (II); a successive movement with considerable rotation of the median phalanx (III); the beginning of a useful rotation of the distal phalanx (IV); a natural successive movement (V); and, finally, the fully closed configuration (VI). Absolute rotation angles θ_1, θ_2 and θ_3 of each phalanx with respect to the palm of the human hand have been evaluated by using Fig. 1 and summarized in Table 1. This natural sequence of closing movement of index human finger has been simulated by using a suitable kinematic model via a computer with the measured angles θ_1, θ_2, θ_3 and dimensions L_1, L_2, L_3 of each phalanx, as shown in Fig. 2. A kinematic model of the index human finger of Fig. 1 has been formulated in order to design a one d.o.f. articulated finger mechanism.

In Fig. 3 the measured rotation angles θ_2 and θ_3 of Table I have been reported *versus* the measured rotation angle θ_1 of the proximal phalanx (Circles show the measured points). Algebraic equations of n-order could be formulated to express the angles θ_2 and θ_3 as functions of θ_1. For example, a least square curve fit could be used as in reference [19]. Consequently, a very good approximation of human finger motion could be obtained. This method can be conveniently aimed to obtain a kinematic synthesis of finger mechanisms, which are composed by across-four bar linkages. On the other hand, these mechanisms can perform only the particular motion for which they have been synthesized.

Greater flexibility can be obtained by means of a one d.o.f. articulated finger mechanism, which is provided with a suitable transmission system from remotely located actuators for each joint. In fact, when a component of the transmission system is substituted, the proposed articulated finger mechanism can perform a different motion. Thus, we have thought it convenient to use a simple linear interpolation of the measured points, as shown in Fig. 3. The following equations have been obtained

$$\vartheta_2 = K_{2H}\vartheta_1 \tag{1}$$

$$\vartheta_3 = K_{3H}\vartheta_1 \tag{2}$$

and gains $K_{2H} = 4.65$ and $K_{3H} = 6.94$ have been evaluated. The linear equations (1) and (2) express the rotations of median and distal phalanges as a function of the rotation angle θ_1 and thus they suggest suitable solutions for the mechanical design of an articulated finger mechanism with one d.o.f. only. It is worth noting that basic mechanical devices, as wires, sprocket chains, belts, timing belts transmission

https://doi.org/10.1017/S0263574701003587 Published online by Cambridge University Press

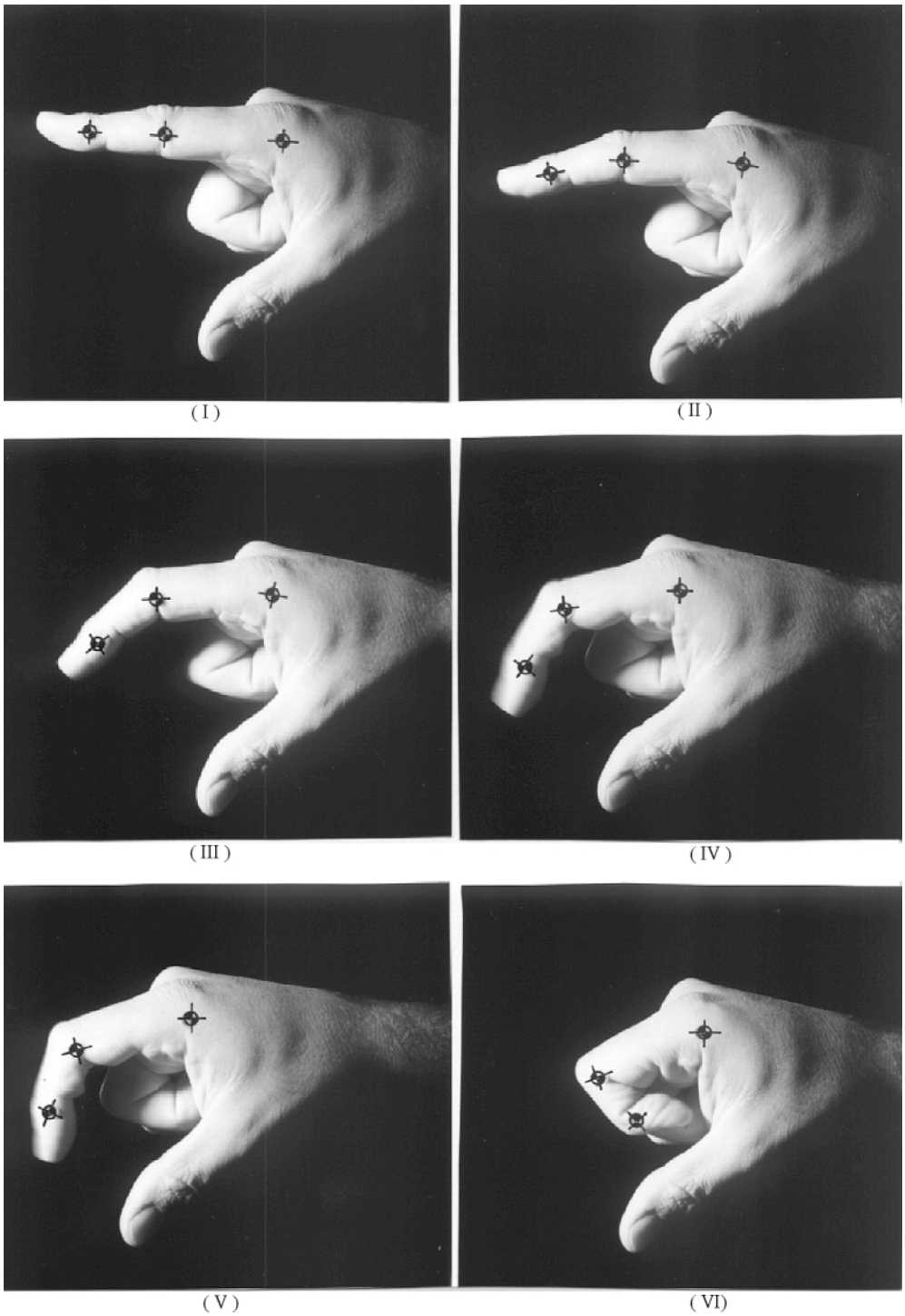

Fig. 1. Natural sequence of a closure action of index human finger: (I) Initial fully extended configuration; (II), (III), (IV), (V) Intermediate configurations; (VI) Final closed configuration.

Table I. Rotation angles θ_1, θ_2 and θ_3 of proximal, median and distal phalanges of index human finger for the configurations I, II, III, IV, V and VI of Fig. 1.

	I	II	III	IV	V	VI
θ_1 [deg]	0	3	6	13	17	27
θ_2 [deg]	0	15	40	60	68	134
θ_3 [deg]	0	20	47	75	98	198

systems or epicyclic gear trains involve constant transmission ratios. Of course, variable transmission ratios can be obtained through non-circular pitch curves, but in this paper we do not take into account this particular case.

When conventional transmission systems are used, a linear function can be obtained between the rotation angles of median and distal phalanges with respect to the rotation angle of the proximal phalanx. Therefore, the gains K_{2H} and K_{3H} can be equivalent to the constant total transmission ratios of the mechanical systems, which transmit the motion

https://doi.org/10.1017/S0263574701003587 Published online by Cambridge University Press

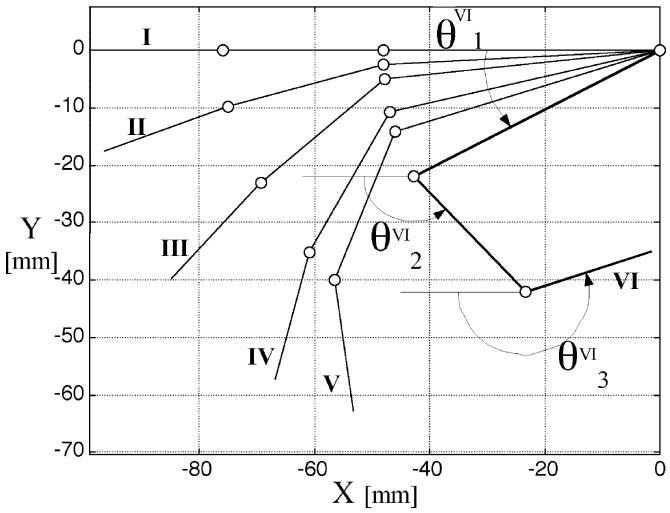

Fig. 2. A model for the configurations of index human finger in the natural sequence of Fig. 1.

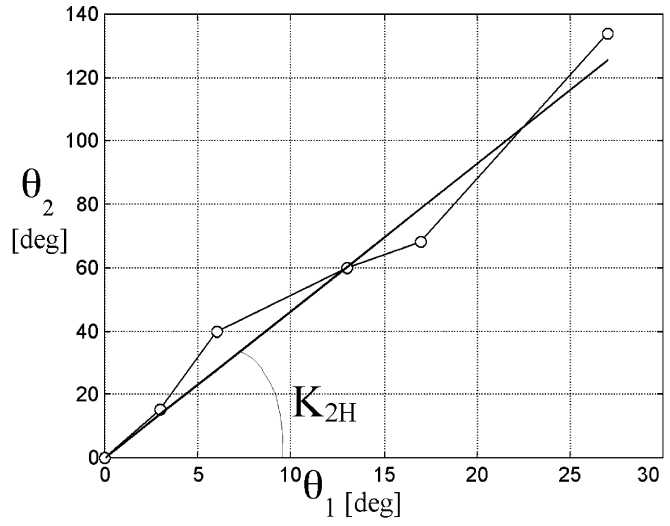

(a)

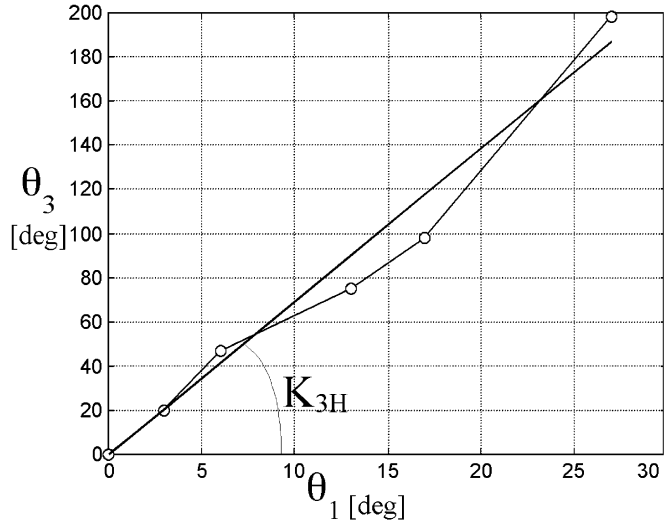

(b)

Fig. 3. Linear interpolation (shown in continuous line) of the measured results (shown by line with circles) of Table I: (a) Rotation angle θ_2 of median phalanx as a function of angle θ_1; (b) Rotation angle θ_3 of distal phalanx as a function of angle θ_1.

to each phalanx. In addition, the interchangeability of transmission system components represents an interesting feature the motion of several fingers.

AN ARTICULATED FINGER MECHANISM

A mechanism for articulated fingers can be synthesized as an open kinematic chain with three links connected by revolute joints. This kinematic chain has three d.o.f.s, which can be operated by means of three independent actuators. Each link corresponds to a phalanx of a human finger. In order to obtain a mechanical prototype very similar to the human finger in terms of weight and shape, actuators are usually installed far away from the actuated joints.[4–8] Nevertheless, a suitable transmission system is required to transmit the motion from the actuators to the corresponding joints of the articulated finger mechanism. This transmission system can be designed by using wires, sprocket chains, belts and timing belts or epicyclic gear trains. From a kinematic viewpoint, these mechanical devices can be considered as equivalent when they are designed in a suitable way.

In fact, Fig. 4 shows kinematic schemes, which correspond to transmission systems using wires, sprocket chains, belts, timing belts and epicyclic gear trains. In particular, the kinematic scheme of Fig. 4(a) shows parallel and cross types of transmission systems between two general wheels, which can be chain sprockets, pulleys, timing pulleys. The parallel type can be obtained using a wire, sprocket chain, belt or timing belt, while the cross type can be obtained by means of a wire or belt only.

Referring to Fig. 4(a), a belt transmission system can be installed on $j1$ and jN wheels with pitch radii R_{j1} and R_{jN}, respectively. Both wheels are joined on the link q, which is connected to the base frame 0. The rotation angles $\theta_{j1,q}$, $\theta_{jN,q}$ of wheels $j1$ and jN are evaluated with respect to link q, while the angles $\theta_{j1,0}$ and $\theta_{jN,0}$ correspond to rotations of these wheels with respect to base frame 0.

Fig. 4(b) illustrates an epicyclic gear train, which is composed by N gears. Each gear is connected to link q through a revolute joint. The pitch radii of gears are

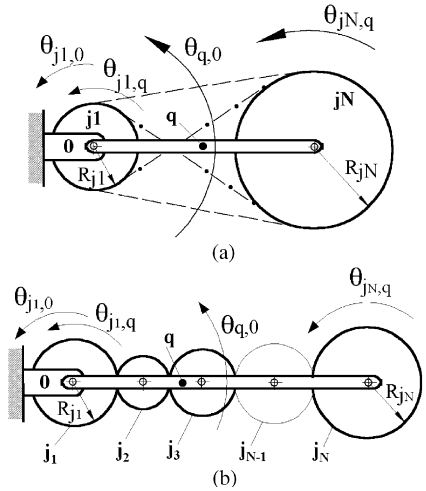

Fig. 4. Kinematic schemes of basic transmission systems, for articulated finger mechanisms: (a) Wire, sprocket chain, belt or timing belt transmission system; (b) Epicyclic gear train.

https://doi.org/10.1017/S0263574701003587 Published online by Cambridge University Press

indicated with $R_{j1}, R_{j2}, \ldots R_{jN}$ and $\theta_{j1,q}, \theta_{j2,q}, \ldots \theta_{jN,q}$ are the corresponding rotation angles with respect to link q. Similarly, angles $\theta_{j1,0}$ and $\theta_{jN,0}$ are the rotation angles of gears $j1$ and jN with respect to the base frame 0. The kinematic analysis of both transmission systems of Fig. 4 can be formulated by

$$\frac{\vartheta_{j1,q}}{\vartheta_{jN,q}} = \pm \frac{R_{jN}}{R_{j1}} \tag{3}$$

where the sign choice gives the opportunity to reverse the rotation of the final element with respect to the first one. In fact, for the kinematic scheme of Fig. 4(a) the sign plus is for a parallel installation of a wire, sprocket chain, belt or timing belt and the sign minus corresponds to crossed types of a wire or belt. For the epicyclic gear train of Fig. 4(b), the sign plus is for an odd number of gears, and the sign minus is for an even number of gears. Equation (3) can be combined into the expression

$$\vartheta_{j1,0} = \vartheta_{q,0} + \vartheta_{jN,q} \tag{4}$$

which expresses the absolute rotation angle of wheel or gear $j1$ as a function of the absolute rotation angle of link q and relative rotation angle of wheel or gear jN.

The kinematic analysis of any open kinematic chain, which is obtained by a serial connecting of the kinematic schemes of Fig. 4, can be formulated in a systematic way by using Eqs. (3) and (4).

The articulated finger mechanism with three d.o.f.s of Fig. 5 has been designed by using the transmission systems of Fig. 4. Assuming the actuators to be installed on the base frame m_0, the articulated finger mechanism can operate as the following: the first phalanx m_1 (proximal) is directly actuated, Fig. 5(a); the second phalanx m_2 (median) is actuated through an epicyclic gear train, which is composed by six gears m_4, m_5, m_6, m_7, m_8, and the last one fixed on m_2, Fig. 5(b); the third phalanx m_3 (distal) is actuated through any transmission system based on wires, sprocket chains, belts, or timing belts between wheels m_9 and m_{10a}, and by means of an epicyclic gear train between gear m_{10b} and gear fixed on m_3. Wheel m_{10a} and gear m_{10b} are rigidly connected between them, but they are both idle about the joint axis connecting median and distal phalanges.

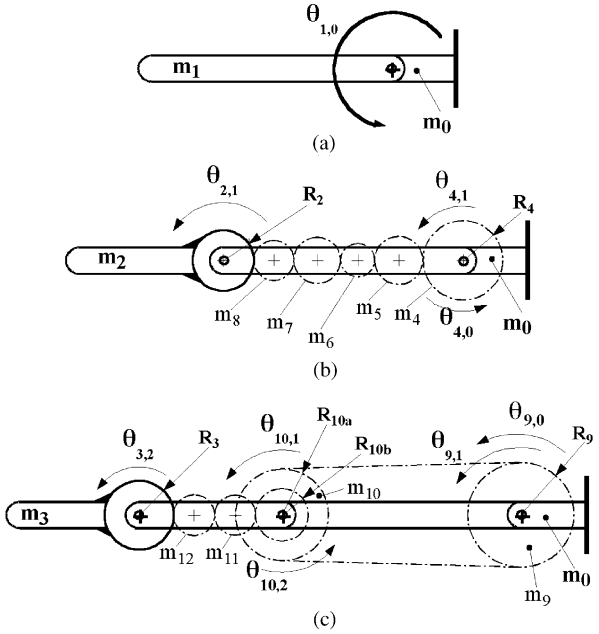

Fig. 5. Kinematic schemes for the proposed three d.o.f.s articulated finger mechanism with actuators installed on the base frame m_0: (a) Direct actuation of proximal phalanx m_1; (b) Epicyclic gear train to move median phalanx m_2; (c) Parallel transmission system of Fig. 4(a) and epicyclic gear train to move the distal phalanx m_3.

Thus, Eqs. (3) and (4) can be expressed in a specific form for each transmission system, which has been used to operate each phalanx of the proposed mechanism of Fig. 5. For the epicyclic gear train of median phalanx Fig. 5(b), it yields

$$\frac{\vartheta_{4,1}}{\vartheta_{2,1}} = -\frac{R_2}{R_4} \text{ and } \vartheta_{4,0} = \vartheta_{1,0} + \vartheta_{4,1} \tag{5}$$

For the parallel transmission system of Fig. 4(a) for distal phalanx, Fig. 5(c), it yields

$$\frac{\vartheta_{9,1}}{\vartheta_{10,1}} = +\frac{R_{10a}}{R_9} \text{ and } \vartheta_{9,0} = \vartheta_{1,0} + \vartheta_{9,1} \tag{6}$$

Similarly, for the epicyclic gear train of distal phalanx, Fig. 5(c), it yields

$$\frac{\vartheta_{3,2}}{\vartheta_{10,1}} = -\frac{R_{10b}}{R_3} \text{ and } \vartheta_{10,1} = \vartheta_{10,2} + \vartheta_{2,1} \tag{7}$$

The above-mentioned Eqs. (5) to (7) can be conveniently grouped in the following matrix formulation

$$\begin{bmatrix} \vartheta_{1,0} \\ \vartheta_{4,0} \\ \vartheta_{9,0} \end{bmatrix} = \begin{bmatrix} 1 & 0 & 0 \\ 1 & -R_2/R_4 & 0 \\ 1 & +R_{10a}/R_9 & -R_{10a}R_3/R_9R_{10b} \end{bmatrix} \begin{bmatrix} \vartheta_{1,0} \\ \vartheta_{2,1} \\ \vartheta_{3,2} \end{bmatrix} \tag{8}$$

which expresses the absolute rotation angles of actuated members m_1, m_4 and m_9 with respect to the base frame m_0 as functions of joint rotation angles of three d.o.f.s articulated finger mechanism of Fig. 5. Equation (10) can be useful for a position and speed control of finger motion when three independent actuators are installed on base frame m_0 to operate the three phalanges m_1, m_2 and m_3 because of wheel m_9 and gear m_4.

However, in order to simplify both actuation and control, the one d.o.f. articulated finger mechanism of Fig. 6 has

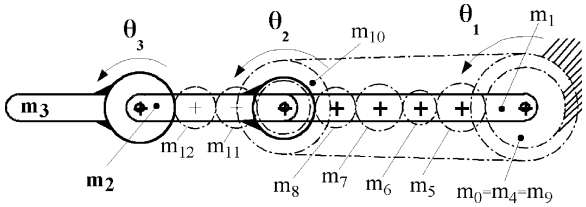

Fig. 6. The proposed one d.o.f. articulated finger mechanism.

https://doi.org/10.1017/S0263574701003587 Published online by Cambridge University Press

been obtained from that of Fig. 5 by assuming gear m_4 and wheel m_9 as fixed to base frame.

This choice gives

$$\vartheta_{4,0} = \vartheta_{9,0} = 0 \tag{9}$$

Consequently, Eqs. (8) and (9) give the coefficients K_2 and K_3 in the form

$$K_2 = 1 + \frac{R_4}{R_2} \tag{10}$$

$$K_3 = \frac{R_9 R_{10b}}{R_3 R_{10a}} + \frac{R_{10b} R_4}{R_3 R_2} + \frac{R_4}{R_2} + 1 \tag{11}$$

These coefficients define the coupling of motion among the three phalanges of the one d.o.f. articulated finger mechanism of Fig. 6. Equations (10) and (11) can be used to calculate different values of K_2 and K_3 by properly sizing the pitch radii of the transmission elements. Consequentially different kinds of closing movements can be obtained. Thus, each pair of K_2 and K_3 values correspond to a specific closing movement of the articulated finger mechanism with characteristics similar to those of the index human finger of Fig. 1.

These coefficients are constant because of constant transmission ratios of the used transmission systems for each phalanx. Thus, they can be assumed as fundamental parameters for designing one d.o.f. articulated finger mechanisms with operation similar to human finger action.

A very convenient practical design can be obtained by choosing equal pitch radii of gears and equal pitch radii of wheels in order to have an easy and compact mechanical design. In this case, Eqs. (10) and (11) give $K_2 = 2$ and $K_3 = 4$. Figure 7 shows the corresponding scheme of the one d.o.f. articulated finger mechanism and the sequence of its configurations for the closing movement. In order to compare its operation with respect to that of index human finger of Fig. 1, each configuration of Fig. 7 corresponds to an input angle θ_1 of Table 1. Thus, comparing the configurations of Fig. 7 with those of Fig. 2, it is worth noting the major closure of human finger for the same rotation angles of the proximal phalanx.

However, the performance of one d.o.f. articulated finger mechanisms can be synthetically evaluated by means of positioning errors that can be computed by referring to the motion analysis results of index human finger in Fig. 1.

In particular, positioning errors ε_2 and ε_3 for the median and distal phalanges, respectively, can be computed as the distance of the phalanx extreme points between the corresponding configurations for the index human finger and articulated finger mechanism as shown in Fig. 8.

For the sake of simplicity, in the following we shall use the subscripts 1, 2 and 3 to indicate the absolute rotation angles of proximal, median and distal phalanges, respectively, instead of 1, 0; 2, 0 and 3, 0.

The positioning errors can be formulated as, Fig. 8,

$$\varepsilon_i = \sqrt{\varepsilon_{iX}^2 + \varepsilon_{iY}^2} \quad (i = 2, 3) \tag{12}$$

when the proximal phalanx is always positioned with an angle θ_1 equal to a human finger configuration. The Cartesian components of the positioning errors can be computed in the form

$$\varepsilon_{iX} = X_i - X_{im} \tag{13}$$

$$\varepsilon_{iY} = Y_i - Y_{im} \tag{14}$$

where X_i and Y_i represent the Cartesian coordinates of extreme points of phalanx i for the articulated finger mechanism, and X_{im} and Y_{im} are the Cartesian coordinates of the corresponding points in the human finger. Thus, X_i and Y_i can be expressed as

$$X_i = -\sum_{p=1}^{3} L_p \cos(K_p \vartheta_1) \tag{15}$$

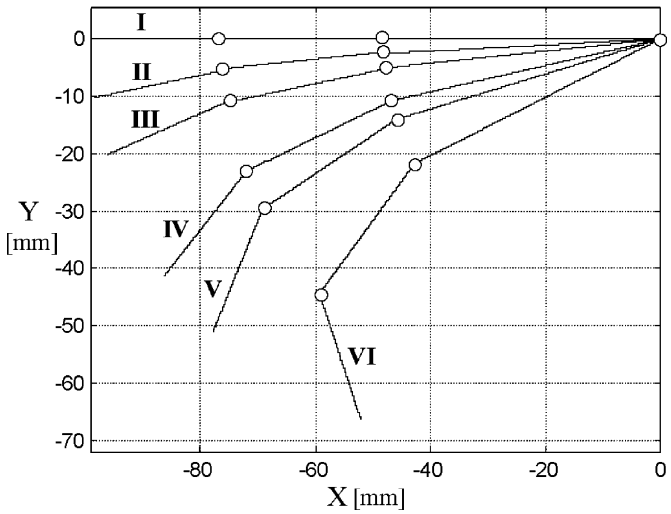

Fig. 7. Sequence of configurations for closing movement of one d.o.f. articulated finger mechanism of Fig. 6 with $K_2 = 2$ and $K_3 = 4$.

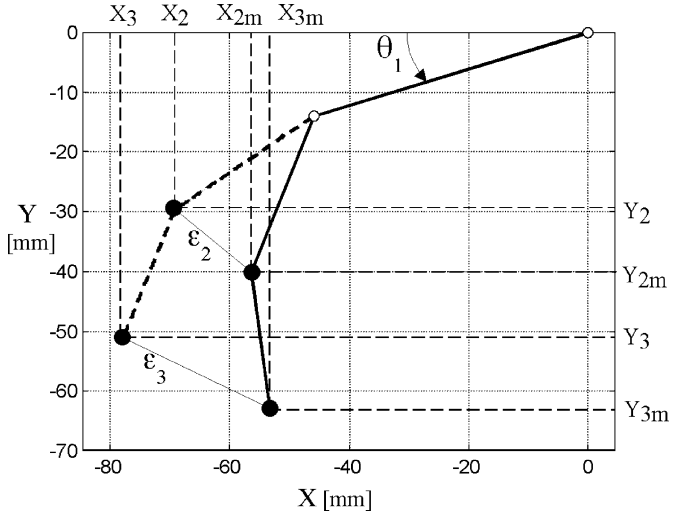

Fig. 8. A scheme to evaluate the positioning errors ε_2 and ε_3 of one d.o.f. articulated finger mechanism with respect to a kinematic model of human finger.

https://doi.org/10.1017/S0263574701003587 Published online by Cambridge University Press

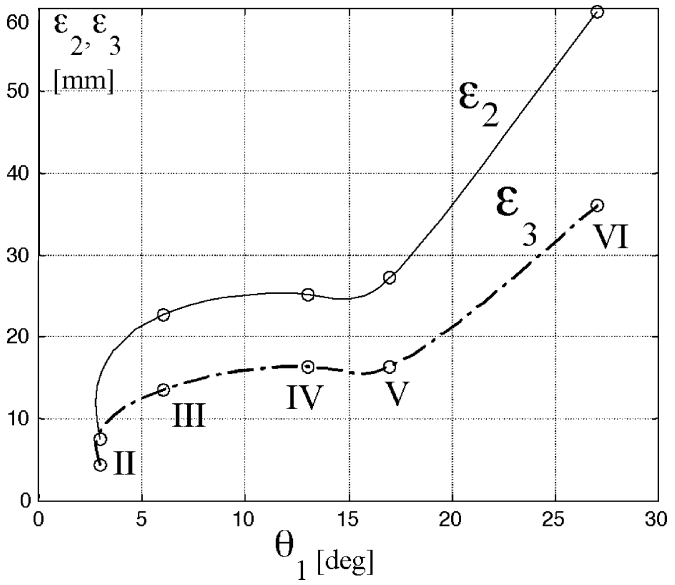

Fig. 9. Positioning errors ε_2 and ε_3 for the one d.o.f. articulated finger mechanism of Fig. 6 with $K_2=2$ and $K_3=4$ as a function of angle θ_1.

$$Y_i = -\sum_{p=1}^{3} L_p \sin(K_p \vartheta_1) \tag{16}$$

By using the measured angles of Table I for the index human finger, X_{im} and Y_{im} can be expressed as

$$X_{im} = -\sum_{p=1}^{3} L_p \cos \vartheta_p \tag{17}$$

$$Y_{im} = -\sum_{p=1}^{3} L_p \sin \vartheta_p \tag{18}$$

where the index $p=1, 2, 3$ corresponds to the proximal, median and distal phalanges, respectively. In particular, $p=1$ gives $K_1=1$ since the trajectory of proximal phalanx extremity coincides with a circle. When the angle θ_1 is assumed as variable parameter, Eqs. (15) and (16) express also the fingertip trajectory of one d.o.f. articulated finger mechanism. The values of the positioning errors ε_2 and ε_3 in Fig. 9 are computed by using the significant five configurations, II to VI, which are shown in Figs. 2 and 7, and interpolating the results by means of two suitable splines.

The computed values can be considered high (the maximum is about 60 mm), but they refer to the human sequence of Fig. 1, which can be considered only a very specific sequence for the closing movement. In addition, the human finger can be thought equivalent to a kinematic chain with three d.o.f.s, but the proposed articulated finger mechanism presents one d.o.f. only.

Nevertheless, the proposed practical design of articulated finger mechanism with $K_2=2$ and $K_3=4$ can be easily improved to mimic the natural closing movement of an index human finger of Fig. 1.

AN ANTHROPOMORPHIC FINGER MECHANISM

It is possible to obtain a one d.o.f. articulated finger mechanism that can mimic satisfactorily the closing movement of the index human finger of Fig. 1 by properly evaluating the coefficients K_2 and K_3.

Of course, the human finger has great capability and it can grasp objects of different sizes and shapes. A one d.o.f. articulated finger mechanism can be thought of as suitable for an *a priori* determined class of objects with a given shape and size.

However, the specific closing movement of Fig. 1 can be obtained by the proposed mechanism of Fig. 6 in a satisfactory approximation when its kinematic design is selected with values $K_2=K_{2H}$ and $K_3=K_{3H}$, which represent the gains of Eqs. (1) and (2), respectively. Thus, we can assume equal pitch radii for all gears, which are installed between the first and last gear of each epicyclic gear train since they have no effects on coefficients K_2 and K_3. Then, one can assume an equal pitch radii of wheels in order to ensure the maximum arc of contact between wire, sprocket chain, belt or timing belt and both wheels. Consequently, the pitch radii R_2 and R_4 of the epicyclic gear train of Fig. 5(b) and the pitch radii R_3 and R_{10b} of the epicyclic gear train of Fig. 5(c) can be calculated by Eqs. (10) and (11) when the lengths of three phalanges are also given.

The synthesized mechanism will operate as shown in the simulation of Fig. 10. Each configuration of Fig. 10 has been obtained for an input angle θ_1 of Table I. A comparison of this articulated finger mechanism with respect to the index human finger is shown in Fig. 11 where the trajectories of the revolute joints are depicted in order to compute the positioning errors ε_2 and ε_3. They have been computed by using Eqs. (12) to (18), and the results are plotted in Fig. 12.

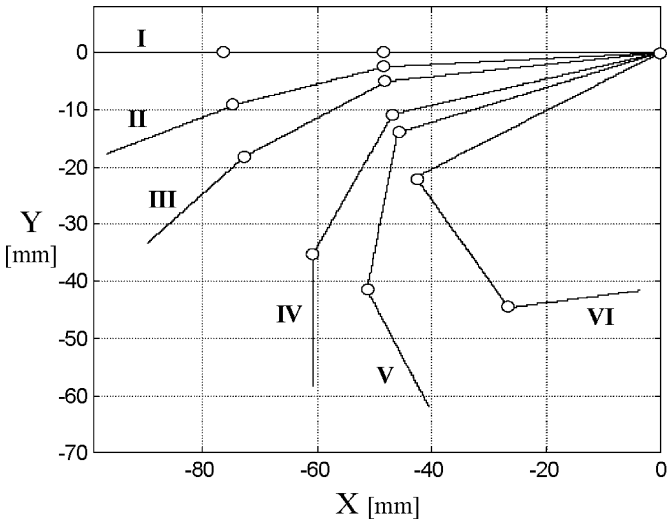

Fig. 10. Sequence of configurations for closing movement of one d.o.f. articulated finger mechanism of Fig. 6 with $K_2=4.65$ and $K_3=6.94$.

https://doi.org/10.1017/S0263574701003587 Published online by Cambridge University Press

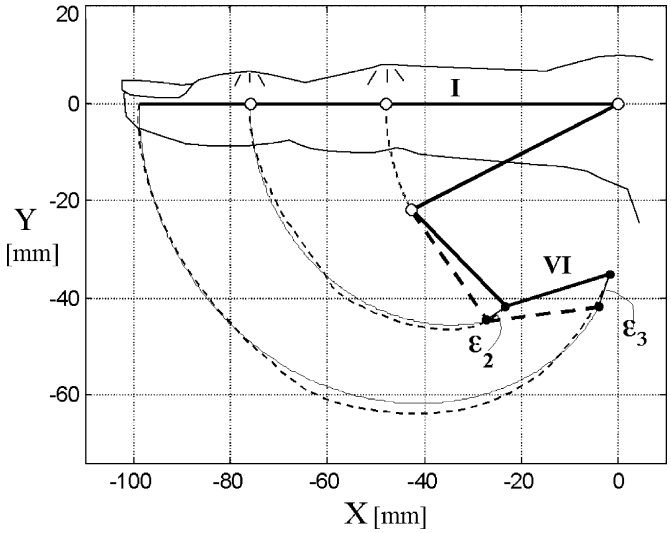

Fig. 11. Trajectories of tip and joints of finger mechanism (dashed line) as compared with spline trajectories for human finger (continuous line).

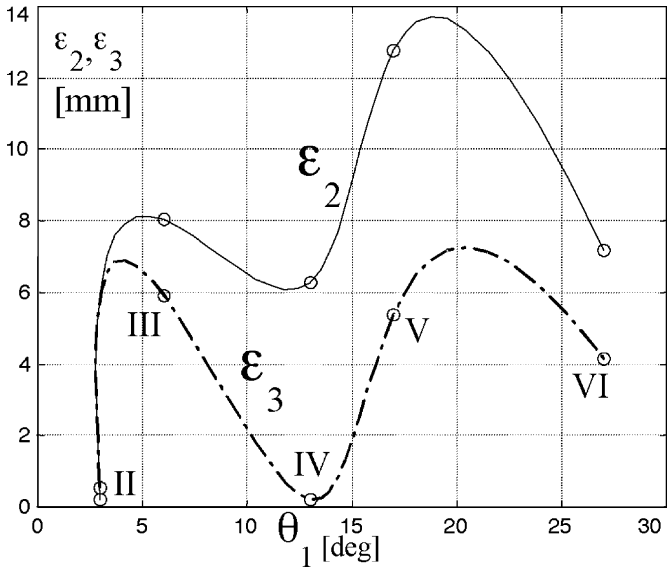

Fig. 12. Position errors ε_2 and ε_3 for the one d.o.f. articulated finger mechanism of Fig. 6 with K_2=4.65 and K_3=6.94 as a function of angle θ_1.

It is worth noting the improvement with respect to the mechanism solution with K_2=2 and K_3=4 of Fig. 9. This proves also to be an opportunity to easily adjust the values of the coefficients K_2 and K_3 with the aim to obtain required configurations and trajectories.

MECHANICAL DESIGN FOR A FINGER PROTOTYPE

A prototype of a one d.o.f. anthropomorphic finger has been built according to the scheme of Fig. 6 at the LARM (Laboratory of Robotics and Mechatronics) in Cassino. A first assembly for the finger prototype has been made by using transmission systems to obtain K_2=2 and K_3=4. We have used spur gears with equal pitch radii and timing belts with equal pitch radii.

Figure 13 shows the specific mechanical design in which a linear actuator is used to obtain an easy control of the input motion with low-cost components. The three phalanges and base frame m_0 with length l_0=100 mm have been built using commercial bars of an aluminum alloy with a rectangular section 10×30 mm. In order to obtain a suitable anthropomorphic design the lengths l_1=90 mm, l_2=54 mm and l_3=45 mm have been assumed for the three phalanges, respectively. A scale factor of about 1.9 has been applied with respect to the dimensions of an index human finger of Fig. 1.

This choice has been carried out in order to obtain an anthropomorphic design and also to reduce the number of gears. In fact, long phalanges require a greater number of gears for the transmission of motion or a bigger size of gears. Normally, it is not convenient to increase too much the number of gears because of the effect of backlash on the positioning errors of finger; in addition, bigger sizes of gears do not ensure an anthropomorphic shape of finger. Thus, we have optimized both effects in order to obtain an anthropomorphic design and low positioning errors.

Ten equal plastic spur gears with module 1 mm and teeth number 18 have been used for the two epicyclic gear trains. Two equal timing pulleys with pitch radii 2 R_9=2 R_{10a}=24.95 mm and teeth number 32 allow the transmission of motion from phalanx m_1 to phalanx m_3 via the idle timing pulley m_{10}. The timing belt with 2.5 mm pitch and 6 mm

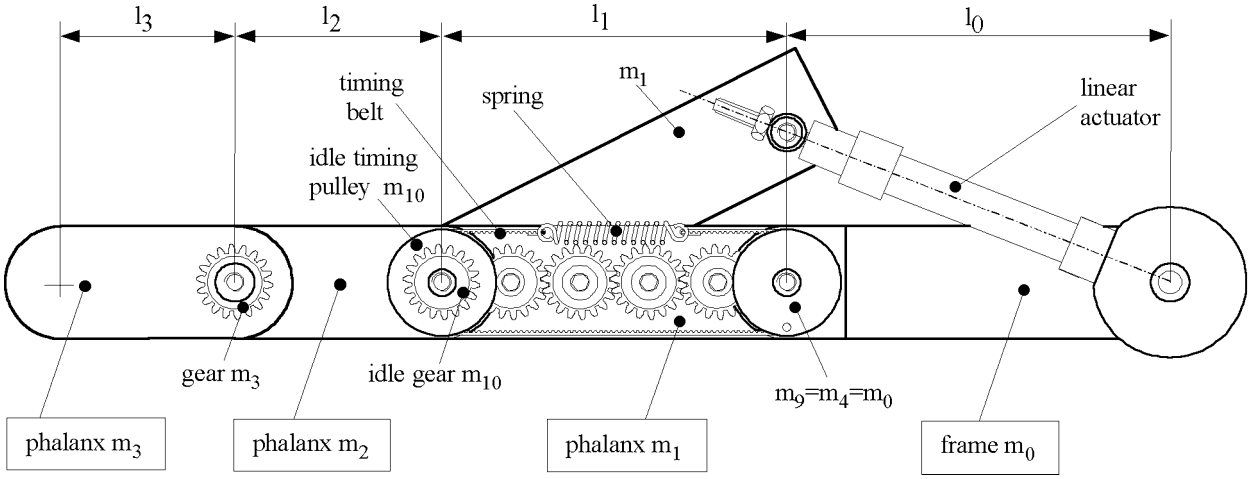

Fig. 13. Mechanical design of the proposed one d.o.f. articulated finger mechanism with low-cost components.

https://doi.org/10.1017/S0263574701003587 Published online by Cambridge University Press

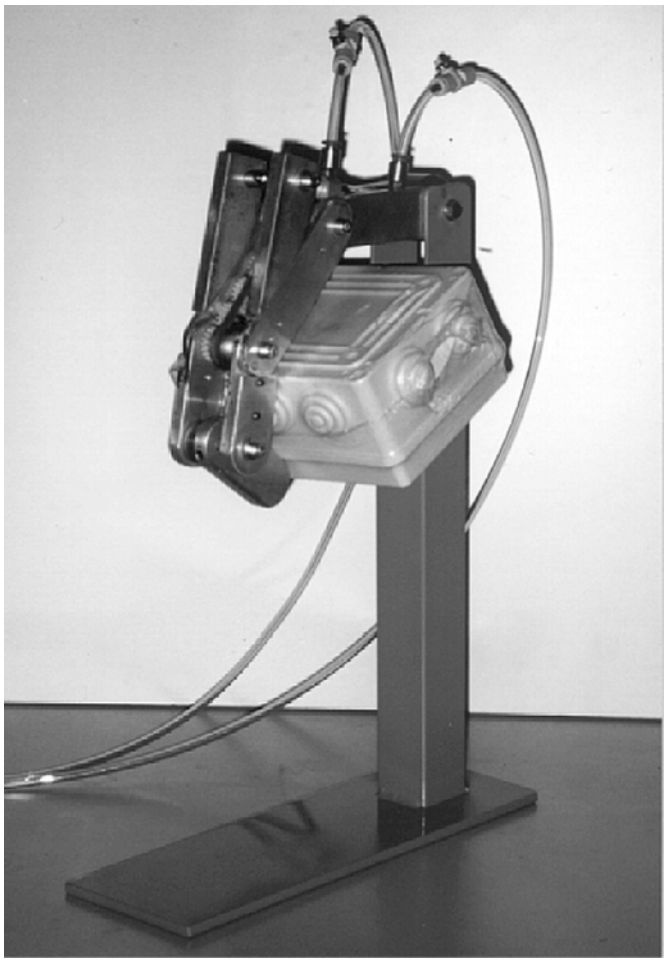

Fig. 14. An experimental test which has been carried out at the Laboratory of Robotics and Mechatronics in Cassino.

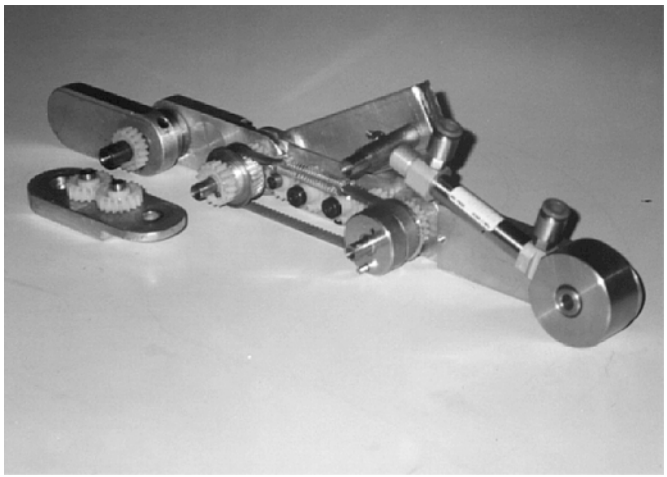

Fig. 15. Assembly of the built prototype with interchangeable gears.

wide has been coupled to both timing pulleys by means of two suitable springs. Figure 14 shows the built prototype during a validation test for the grasp efficiency at LARM in Cassino. A box has been grasped firmly in order to prove the efficiency of the closing configuration for the grasp of objects of different shapes.

The flexibility of the proposed mechanical design for transmission systems can be verified by looking at Fig. 15 where the easy assembly of the elements is shown.

Indeed, the proposed prototype will be used in the near future for the experimental validation of several solutions of transmission systems by changing gear sizes and also with the aim to investigate aspects of the mechanics of grasp.

CONCLUSIONS

In this paper a design for anthropomorphic fingers is proposed as based on the characteristics of a closing movement of an index human finger. An articulated finger mechanism has been proposed and suitable transmission systems have been designed for both three and one d.o.f.s solutions by using low-cost components and a compact mechanical design. Main attention has been given to the one d.o.f. articulated finger mechanism that can mimic satisfactorily the analyzed motion of a human finger. The basic kinematics has been investigated also with the aim to develop future improvements of the mechanical design and grasp behavior, even for human prosthesis.

References

1. C.L. Taylor and R.J. Schwarz, “The Anatomy and Mechanics of the Human Limbs”, *J. of Artificial Limbs*, **2**, 22–35 (1955).
2. M.R. Cutkosky, “On Grasp Choice, Grasp Models, and the Design of Hands for Manufacturing Tasks”, *IEEE Transactions on Robotics and Automation*, **5**, No. 3, 269–279 (1989).
3. T. Iberall, “Human Prehension and Dexterous Robot Hands”, *Int. J. Robotics Research* **16**, No. 3, 285–299 (1997).
4. A. Rovetta, “On Biomechanics of Human Hand Motion in Grasping: A Mechanical Model”, *Mechanism and Machine Theory* **14**, 25–29 (1979).
5. S. Hirose and Y. Umetani, “The Development of a Soft Gripper for the Versatile Robot Hand”, *Mechanism and Machine Theory*, **13** 351–359 (1978).
6. J.K. Salisbury, “Design and Control of an Articulated Hand”, *International Symposium on Design and Synthesis*, Tokyo (1984), pp. 459–466.
7. S.C. Jacobsen, J.E. Wood, D.F. Knutti and K.B. Biggers, “The Utah/M.I.T. Dextrous Hand: Work in Progress”, *Int. J. Robotics Research* **3**, No. 4, 21–50 (1984).
8. C.M. Gosselin, S. Montambault and C.J. Gosselin, “Manus Colobi: Preliminary Results on the Design of a Mechanical Hand for Industrial Applications”, *19th ASME Design Automation Conference*, Albuquerque (1993), **DE-Vol. 65–1**, 585–592.
9. G.R. Dunlop and D.K. Ward, “The Kinematics of a Fifteen DOF Fingered Hand”, *Ninth IFToMM World Congress on the Theory of Machines and Mechanisms*, Milano (1995) **3**, pp. 2249–2253.
10. J. Butterfass, G. Hirzinger, S. Knoch and H. Liu, “DLR’s Multisensory Articulated Hand Part I: Hard- and Software Architecture”, *IEEE International Conference on Robotics and Automation*, Leuven (1998), pp. 2081–2093.
11. T. Laliberté and C.M. Gosselin, “Simulation and Design of Underactuated Mechanical Hands”, *Mechanism and Machine Theory* **33**, No. 1/2, 39–57 (1998).
12. C.M. Gosselin and T. Laliberté, *US Patent 5762390* (1998).
13. G. Guo, X. Qian and W.A. Gruver, “A Single-DOF Multi-Function Prosthetic Hand Mechanism with an Automatically Variable Speed Transmission”, *23rd ASME Biennial Mechanisms Conference*, Phoenix (1992), **DE-Vol. 45**, pp. 149–154.

https://doi.org/10.1017/S0263574701003587 Published online by Cambridge University Press

14. G. Figliolini and M. Ceccarelli, "A Mechanical Design of an Articulated Finger Mechanism", *XII Spanish National Conference of Mechanical Engineering*, Bilbao (1997) **3**, 259–266.
15. G. Figliolini, "Fixed and Moving Polodes for a New Articulated Finger Mechanism", *6th International Workshop on Robotics in Alpe-Adria-Danube Region*, Cassino (1997), pp. 319–324.
16. G. Figliolini and M. Ceccarelli, "A Motion Analysis for One D.O.F. Anthropomorphic Finger Mechanism", *25th ASME Biennial Mechanisms Conference*, Atlanta (1998), Paper DETC98/MECH-5985.
17. G. Figliolini and M. Ceccarelli, "Epicyclic Gearings and Timing Belts for an Articulated Finger", *4th World Congress on Gearing and Power Transmission*, Parigi (1999), **3**, pp. 2533–2538.
18. S.E. Baek, S.H. Lee and J.H. Chang, "Design and Control of a Robotic Finger for Prosthetic Hands", *IEEE/RSJ International Conference on Intelligent Robots and Systems*, Kyongju (1999), **Vol. 1**, pp. 113–117.
19. G. Guo, T.T. Lee, W.A. Gruver and J. Zhang, "Design of a Planar Multijointed Prosthetic Finger Mechanism", *21st ASME Biennial Mechanisms Conference*, Chicago (1990), **DE-Vol. 26**, pp. 165–170.
20. J. Zhang, G. Guo and W.A. Gruver, "Optimal Design of a Six-Bar Linkage for an Anthropomorphic Three-Jointed Finger Mechanism", *23rd ASME Biennial Mechanisms Conference*, Phoenix (1992), **DE-Vol. 45**, pp. 299–304.

https://doi.org/10.1017/S0263574701003587 Published online by Cambridge University Press